Electronic structure of ultrathin Ge layers buried in Si(100)

P. O. Nilsson
Department of Physics, Chalmers University of Technology, SE-412 96 Göteborg, Sweden

S. Mankefors
Department of Informatics and Mathematics, University of Trollhättan/Uddevalla, Box 957, SE-461 29 Trollhättan, Sweden

J. Guo and J. Nordgren
Physics Department, Uppsala University, Box 530, SE-751 21 Uppsala, Sweden

D. Debowska-Nilsson
Institute of Physics, Jagellonian University, ul. Reymonta 4, PL-30-059 Krakow, Poland

W.-X. Ni and G. V. Hansson
Department of Physics and Measurement Technology, Linköping University, SE-581 83 Linköping, Sweden
(Received 5 March 2001; published 24 August 2001)

Ultrathin Ge wetting layers, buried in Si(100), have been investigated by soft x-ray emission spectroscopy. With the assistance of *ab initio* density functional theory calculations the electronic structure of the layers could be established. In particular Si bulk states, splitted and resonating in the Ge layers, were identified.

DOI: 10.1103/PhysRevB.64.115306 PACS number(s): 68.35.−p, 71.15.Mb, 71.20.Nr, 78.70.En

I. INTRODUCTION

During the last decades various growth technologies have proven to be powerful methods to produce high-quality epitaxial thin film materials. The techniques include, e.g., molecular beam epitaxy (MBE) and chemical vapor deposition (CVD). In particular high-performance electronic device-oriented materials have been fabricated, such as structures for heterojunction bipolar transistors, field effect transistors, and light emitting diodes.

A fundamental research area of current interest concerns the lattice-mismatched Si/Ge system. Depending on the growth conditions Ge islands or wetting layers are formed on the Si(100) substrate.[1–3] The atomic structure of such systems after capping with Si has been investigated by various means, e.g., transmission electron microscopy (TEM) (Ref. 3) and high-resolution x-ray diffraction[4] (HRXD). Except for localized quantum well or quantum dot states as probed in photoluminescence,[3] the electronic structure is, however, still largely unknown because traditional spectroscopies (e.g., photoelectron and Auger spectroscopies) are too surface sensitive to detect truly buried interfaces. It should in this connection be stressed that it is in general not representative to use thin caplayers because modifications of the buried interface can take place during the overgrowth.[5] We have, however, demonstrated[6–12] that it is feasible to analyze the electronic structure of deeply buried ($\geqslant$10 nm) layers using soft x-ray emission (SXE) spectroscopy. Combined with *ab initio* density functional theory (DFT) calculations fine details in the partial, local density of states of buried layers can be extracted.

We have earlier studied a group IV/II-V semiconductor structure [Si in GaAs (Refs. 6–9)] and a II-V/III-V structure [AlAs in GaAs (Refs. 9–12)]. We complete a systematic series of study here by investigating a group IV/IV structure, namely, Ge in Si.

II. EXPERIMENTAL

Three samples were prepared, namely with 1, 2, and 3 monolayers (ML) of Ge buried in Si(100). The samples were grown in a vacuum generators V-80 MBE system with a base pressure of $<10^{-10}$ Torr.[13] A Si(100) wafer was first cleaned by heating at 800 °C to remove a thin protection oxide. Immediately thereafter a 70-nm thick undoped Si buffer was grown at 700 °C. This substrate was then cooled down to about 275 °C for the deposition of 1, 2, or 3 ML of Ge. Finally a 10-nm thick Si caplayer was grown during which the substrate temperature was increased from 275 to 350 °C.

The surface morphology of the Ge layer was monitored during the growth using reflection high energy electron diffraction (RHEED). All three samples surfaces showed a 2×1 surface reconstruction. For the 3 ML sample the RHEED intensity of the reconstruction spots was a bit weaker than that for the 1 and 2 ML samples. There was, however, no indication of a rougher surface in the meaning that we did not observe traces of a Si bulk diffraction pattern.

The soft x-ray emission experiments were performed at beamline 7.0 of the Advanced Light Source (ALS) at Lawrence Berkeley National Laboratory. The base pressure in the analysis chamber was 1×10^{-9} Torr. The beamline uses a 5-m long, 5-cm period undulator and a spherical-grating monochromator to produce intense and high-resolution soft-x-ray radiation.[14] The monochromator provides a choice of three different spherical gratings. In the present experiment, a 150 lines/mm grating was chosen to give a monochromator resolution of 0.3 eV at 145 eV photon

energy. The refocusing mirrors are capable of focusing the radiation to a small spot size on the sample. This is important because the grazing incidence spectrometer used to record the x-ray emission has a very small acceptance angle. Soft-x-ray fluorescence spectra were recorded using a high-resolution grazing-incidence grating spectrometer.[15] The spectrometer provides a choice of three different spherical gratings. It has also an adjustable entrance slit and a two-dimensional multichannel detector, which can be translated to the focal position defined by the Rowland circle of the grating in use. The 300 lines/mm grating was selected here which provides a spectrometer resolution of 0.5 eV.

Because the observed experimental spectral features were so weak from the buried Ge monolayer samples, we had to verify that the observed features are related to the sample and not to the instrumentation. A reference sample SiC was selected to be measured under the same experimental conditions. The spectrum was found to be very smooth in the energy region 100–140 eV and showed only a minor feature around 122 eV, of no importance for the present work. Thus these experimental observations rule out feature contributions from the instrumentation including detector and electronics.

III. THEORY

The electronic structure of the buried Ge layers were calculated *ab initio* within the density-functional theory (DFT) (Refs. 16 and 17) using the local density approximation (LDA).[18,19] Nonlocal, fully separable pseudopotentials were employed[20,21] to describe the ion-electron interactions. Both the Si and Ge potentials were obtained by self-consistent calculations on free atoms using the relativistic Dirac equation.[22–24] To model the embedded Ge layers, Si slabs with one, two, or three monolayers of Ge were periodically repeated, making up a superlattice in each case. In this way unit supercells were created and an ordinary plane wave based band structure code could be employed.[25,26] The plane-wave cutoff energy was chosen to 16 Ry which returned very good results in a similar investigation for III-V semiconductors.[27] The wave functions were sampled at 15 special Monkhorst **k** points in the irreducible Brillouin zone for each superlattice. This corresponds to 160 points in the full zone. The theoretical values of the lattice constants were used for Ge (5.58 Å) and Si (5.39 Å) everywhere in the calculations.

The 1, 2, and 3 monolayers of Ge were placed centrally inside slabs containing 7, 10, and 9 monolayers of Si, respectively. In the case of 1 ML Ge we used three different geometries to model the buried layer in order to investigate different degrees of mixing between Ge and Si atoms: (i) a single homogenous Ge layer where all Ge atoms are found within the layer, (ii) a 2×2-interface cell where every fourth Ge atom is displaced one atomic layer into the Si slab, and (iii) a 2×2-interface cell with a 50% mix, i.e., every second Ge atom is displaced one layer into the Si slab. Each atomic layer was presumed to have the same interface area as in the bulk Si and all atoms were relaxed. Equilibrium was considered established when all forces were smaller then 0.005 eV/Å, corresponding to an estimated numerical uncertainty of maximum 0.05 Å. Further, in the very thin layers considered here, the in-plane Ge atomic positions were assumed to fully adapt to the symmetry in the host Si lattice. We make this assumption since there is no evidence in the sample of dislocations or high concentration of defects. This means that the Ge layers are strained by 3.5% parallel to the interface. The superlattice constant perpendicular to the interface was, however, optimized with regards to the total energy by calculating the total energy for different *z*-lattice constants in steps of 0.15 Å. The energy dependence was subsequently interpolated by a third degree Legendre polynom in each case and the minimum extracted. Using this method all artificial vertical strain is avoided. In the case of 1 ML Ge, the above procedure was only applied to the homogenous Ge layer though and the unmixed superlattice constant used also for the mixed geometries. The strain introduced into the mixed systems because of this should be, however, very small (see below).

To separate effects from strain and hybridization (see further below) we recalculated the unmixed 1 ML system with all Si atoms exchanged to Ge atoms using the same numerical conditions as above. The atomic positions from the Si(Ge) system were all kept fixed, however, and the supercell dimensions were unchanged. The partial density of states (PDOS) was only calculated for the original buried Ge layer since this was the subject of interest.

It is very important to test the reliability of the computational results. In particular one should find out if the chosen thicknesses of the Si layers are large enough to obtain converged results.

In the first test we investigated the PDOS and the atomic positions in the central layer of pure Si slabs. In all cases very good agreement with the bulk PDOS was achieved. The atomic positions agreed with those in bulk Si within 0.03 Å, despite the large displacements at the surfaces of the slab.

As a second test we redid the calculations for the 1 ML system using a slab of 11 ML of Si at a cutoff energy of 8 Ry since this has proven to give reasonable results for semiconductor systems before[27] what concerns atomic positions and energy differences. Taking into account the differences due to the lower cutoff energy, no relative changes outside the numerical uncertainty were found for either the PDOS, atomic forces, or positions. We also optimized the superlattice constant for the mixed geometries, using 7 ML of Si and an 8 Ry cutoff energy without finding any numerically significant differences with the homogenous unmixed geometry.

A third test aimed at possible errors due to the use of pseudopotentials and the LDA. In an earlier publication[10] on similar systems we made comparisons with other computational schemes not relying on the mentioned approximations. Good agreement was found and there is thus no reason to suspect any errors due to the choice of numerical method.

The PDOS contributions (*s*, *p*, and *d*) were calculated by first extracting the contribution in each specific **k** point and then integrating the **k** space by a Monte Carlo method. A second-degree three-dimensional polynomial interpolation of 27 **k** points lead to a numerical accuracy (for peak positions, intensities, etc.) better than 0.5%.

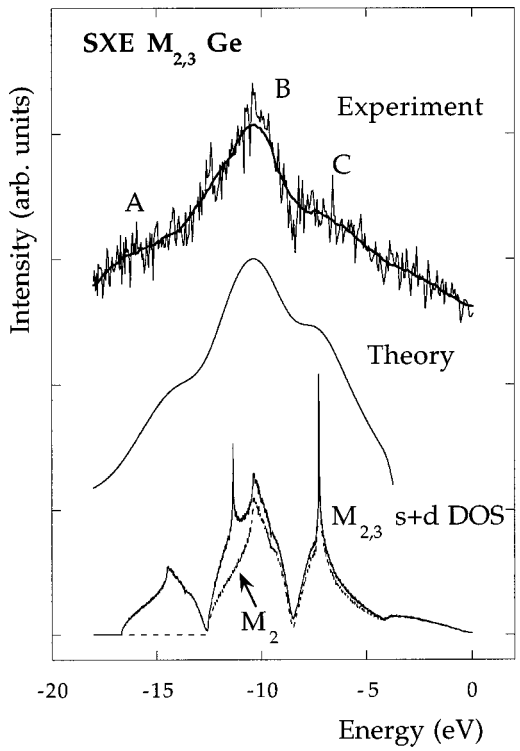

FIG. 1. Experimental and theoretical $M_{2,3}$ SXE spectra from bulk Ge. A Gaussian (0.5 eV) and Lorentzian (2.0 eV) broadening have been applied to the experimental spectrum. For comparison the M_2 and $M_{2,3}(s+d)$ densities of states for the valence band is also shown. The energy scale has been set to zero at the valence band maximum in the M_2 DOS and at the M_2 threshold in the SXE spectra.

The SXE spectra were calculated in a one-electron approximation using the basic theory in Refs. 28 and 29. The photon distribution in the dipole approximation can be written as

$$I(h\nu)\sim(h\nu)^3\int |\langle\phi_c|\mathbf{e}\cdot\mathbf{r}|\phi_\nu\rangle|^2\delta(E_\nu(\mathbf{k})-E_c-h\nu)d^3\mathbf{k},$$

where c and v refer to the core state and the valence band, respectively. The core state wave function ϕ_c was obtained from a linear muffin-tin orbital (LMTO) calculation and its energy was chosen to be the experimental one. The experiment is largely angle integrated so we have summed over all directions of the electromagnetic field **e**.

IV. RESULTS AND DISCUSSION

Bulk Ge was studied as a reference. A recorded emission spectrum, and an arbitrarily smoothed version of it, are shown at the top in Fig. 1. Three peaks A, B, and C are observed. The theoretical spectrum has been convoluted by a Gaussian (0.5 eV) to simulate the experimental broadening and a Lorentzian (2.0 eV) to simulate the lifetime broadening. The resulting spectrum shows the observed three peaks. As our aim is to identify the origin of the structures, our result is satisfactory and we have not tried to optimize broadening parameters, background subtractions, etc. For analysis

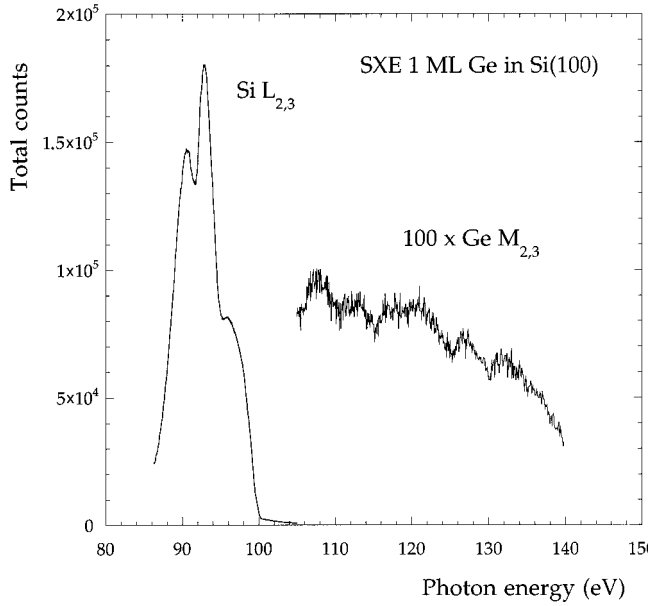

FIG. 2. The recorded SXE spectrum from a Si(100) sample containing 1 ML Ge at a depth of 10 nm.

of the nature of the peaks we have plotted in Fig. 1 the $s+d$ partial density of valence states corresponding to $M_2(3p_{1/2})$ and $M_3(3p_{3/2})$ emissions, respectively. We have assumed an energy separation of 4 eV between the M_2 and M_3 thresholds. A M_2/M_3 intensity ratio of 2.0 was used which is somewhat larger than the statistical ratio 1.5. We find that the lower and upper peaks in the experimental spectrum are solely due to M_3 and M_2 emissions, respectively, while the middle peak is a sum of these two contributions. We will therefore mainly use the low binding energy part for analysis of the Ge layers.

Figure 2 shows experimental emission spectra from a sample containing 1 ML Ge buried 10 nm below a Si(100) surface as described above. We observe that the Ge $M_{2,3}$ emission is about a factor 100 weaker then the Si$L_{2,3}$ emission. In addition to the small volume of the Ge layer, the relatively lower fluorescence yield from the *M* shell, than the *L* shell, is a contributing factor for this intensity difference.

Figure 3 shows calculated $(s+d)$ DOS for various modifications of a buried monolayer of Ge in Si(100). For identification of the features in these curves the $(s+d)$ DOS for bulk Si and Ge have also been plotted. The shapes of these curves are very similar while the energies of the various features are displaced. The main difference between Ge and Si is that Ge has a deeper potential of roughly 1 eV. For Ge-Si substitutionally disordered alloys this fact leads to a ''virtual crystal'' model which assumes a common, average potential, resulting in a common band structure. The question now arises to what extent this model is also valid for a Ge monolayer in a Si crystal. In other words, do the Ge atoms form ''their own'' (resonant) electronic states or are common ''virtual'' Si-Ge states established?

The bulk DOS of Si and Ge display three features, each labeled S_1, S_2, S_3, and G_1, G_2, and G_3, respectively. The 1 ML spectrum (''0% mix'') shows six features. It appears that the G_1 state is split into two states G_1^{xy} and G_1^z and

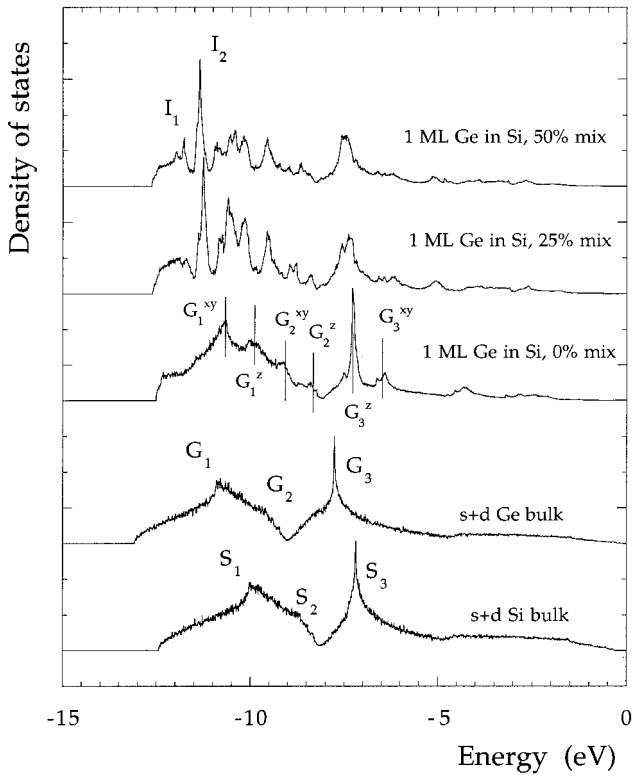

FIG. 3. Calculated $(s+d)$ DOS of 1 ML Ge buried in Si(100). The model for the Si/Ge mixing is explained in the text under ''theory.'' For comparison the $(s+d)$ DOS for bulk Si and Ge are also shown.

similarly happens for G_2 and G_3. The reason for the splitting is the changed symmetry in the Ge layer. According to above bulk Ge has a larger lattice constant (5.58 Å) than bulk Si (5.39 Å) and the epitaxial Ge monolayer is therefore compressed within its plane. As there is a tendency to keep the unit volume unchanged the Ge-Si spacing perpendicular to the plane (z direction) increases by 3.5% (see above), which is somewhat lower than that required for a constant unit volume. The monolayer Ge atoms are thus surrounded by a tetragonal, instead of the bulk cubic structure. The s states are, however, not directly influenced by this effect. On the other hand, the three p levels, degenerate in cubic symmetry, are split, creating two degenerate levels directed within the monolayer plane (x,y) and one level directed perpendicular (z) to the monolayer plane. As we have a mixing of s and p states in the solid, the crystal field splitting of the p states will be reflected indirectly also in the s states, which are observed in the $M_{2,3}$ SXE spectra.

To test this geometrical argument we have recalculated the $(s+d)$ DOS of the buried Ge layer, but with the Si atoms substituted by Ge atoms, keeping all the previous distances unchanged. Indeed we find, as summarized in Fig. 4, that the low-lying peak G_1 in bulk Ge splits into two peaks $G_1'^{xy}$ and $G_1'^{z}$ in the Ge monolayer. The peaks G_2 and G_3 are similarly split. This shows that the splitting of the levels in the Ge layer in bulk Si is a geometrical effect. A further shift of the levels occur due to hybridization between the Ge and Si states, as illustrated in Fig. 4.

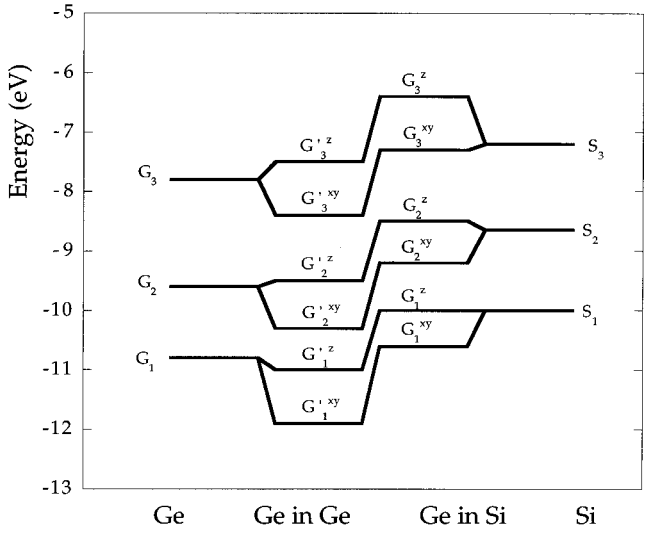

FIG. 4. Theoretical energy level diagram for electronic states in bulk Ge, buried strained Ge layer in bulk Ge(100) (see under ''theory''), Ge layer in bulk Si(100) and bulk Si.

In the real system the Ge atoms will not form a perfect smooth monolayer, but due to intermixing the Ge atoms will, to some extent, occur on neighboring Si sites. As described above in the theoretical section this situation has been simulated by two calculations labeled in Fig. 3 ''25% mix'' and ''50% mix,'' respectively. On the whole the two spectra are quite similar. Entirely new, complicated structure appears, however, as compared to ''0% mix,'' which will not be analyzed here. We note, however, that two new strong peaks appear in the 11–12 eV region (I_1 and I_2), i.e., below any structure in the ''0% mix'' spectrum.

The experimental spectra were convoluted with a Gaussian function. The width (0.3 eV) was optimized so that the statistical noise was washed out, but that all significant structures remained. A comparison between the experimental 1 ML Ge $M_{2,3}$ emission spectrum and the theory discussed above is shown in Fig. 5. In the low-lying region (about 4 eV wide) we can make a direct comparison between theory and experiment as only M_3 emission contributes there. The experimental spectrum shows six peaks in this region. Since the theoretical SXE spectra resembles the local $(s+d)$ DOS very closely for all systems we have chosen to use the PDOS rather than the spectra for simplicity. The theoretical $(s+d)$ partial density of states for a perfect and a ''25% mixed'' monolayer of Ge in Si bulk are plotted to identify the origin of the structures in the spectrum. The four high-energy experimental peaks can be directly associated with the G_1^{xy}, G_1^z, G_2^{xy}, and G_2^z peaks in the perfect monolayer (see also Fig. 3), while the two low energy peaks have no counterparts. The theory for mixed monolayers shows however structure in this region. As seen in Fig. 5, the structures I_1 and I_2 are likely to be responsible for the two low-energy peaks. Analysis shows that the structures I_3 and I_4 can also be identified in the experimental curve. One should, however, note that perfect agreement with the ''mixed'' theory is

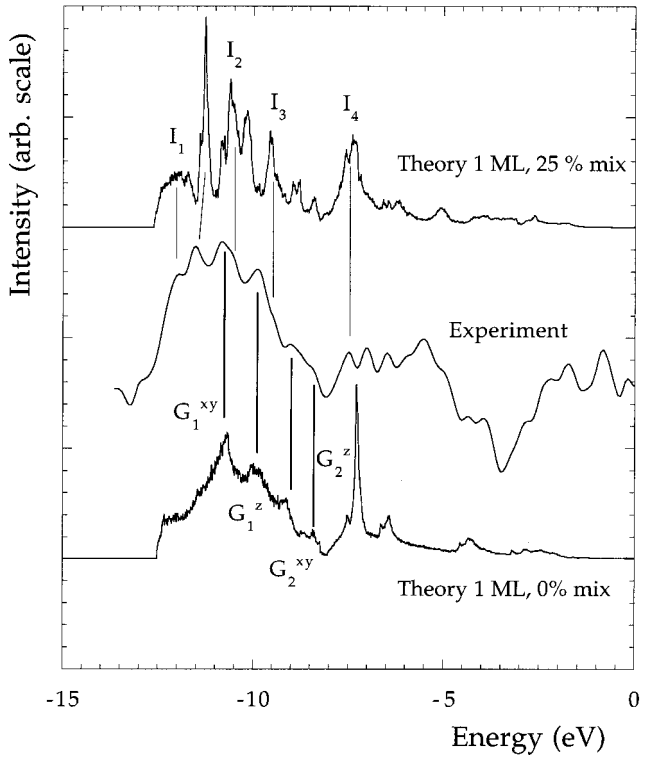

FIG. 5. Comparison between experimental SXE spectra and $(s+d)$ DOS theory for 1 ML Ge in Si(100). The experimental spectrum has been convoluted by 0.3 eV Gaussian. The theoretical curves are taken from Fig. 3.

not expected because of the approximate model (see theory section above). Our observations show, however, clearly that the one monolayer Ge is almost perfect, but that there is some mixing present.

Samples with 2 and 3 ML of Ge in Si(100) were also studied. The experimental results are displayed in Fig. 6(a). The 1, 2, and 3 ML spectra show some overall agreement, but the details differ vastly. Figure 6(b) shows the theoretical $s+d$ DOS for the three systems. We have not computed the effects of intermixing for 2 and 3 monolayers though and we can therefore not make a detailed analysis of the experimental spectra here. We can point out, however, that there is a great deal of resemblance between theory and experiment. The two low-energy peaks for 1 ML, indicated in Fig. 6(b) by G_1^{xy} and G_1^z, go away (or are possibly displaced) for 2 and 3 ML. The same behavior is reproduced in the calculations shown in Fig. 6(b).

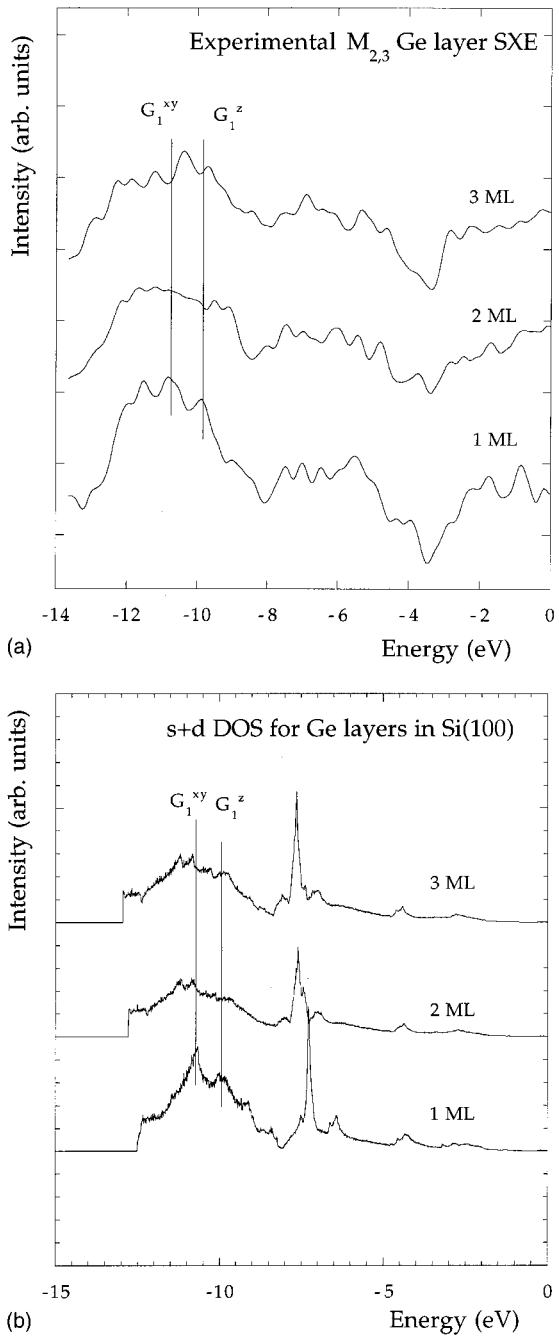

FIG. 6. (a) Experimental $M_{2,3}$ SXE spectra for 1, 2, and 3 ML of Ge buried 10 nm below a Si(100) surface. The energy is normalized relative the M_3 threshold. The labeled peaks are the same as in Figs. 3 and 5. (b) Local, partial $(s+d)$ density of states calculated for 1, 2, and 3 ML of Ge buried in Si(100). The labeled peaks are the same as in Figs. 3 and 5.

V. CONCLUSIONS

We have studied the electronic structure of 1, 2, and 3 ML of Ge buried in Si(100) using SXE spectroscopy and *ab initio* DFT computations. There is very good agreement between experiment and theory, in particular for the case of 1 ML Ge.

There is a strong indication that the layers are highly perfect, but that some intermixing with the neighboring Si atoms occurs. The electronic states in the Ge layer can be viewed as the Si bulk states tunnelling through the Ge layer and resonating on the Ge atoms. Thus the situation resembles the ''virtual crystal approximation'' for alloys, where an averaged electronic structure is observed. Due to the reduced symmetry in the Ge layer two Ge resonances are observed for each Si bulk state. This is illustrated in Fig. 4 where the S_n states are seen to split into G_n^{xy} and G_n^z states.

ACKNOWLEDGMENTS

This work has been supported by the Swedish Natural Science Research Council (NFR) and the Swedish Research Council for Engineering Sciences (TFR). D. D.-N. acknowledges financial support from the Swedish Institute. The experimental work at ALS, Lawrence Berkeley National Laboratory was supported by the U.S. Department of Energy under Contract No. DE-AC03-76SF00098.

[1] G. Capellini, L. Di Gaspare, F. Evangelisti, E. Palange, A. Notargiacomo, C. Spinella, and S. Lombardo, Supercond. Sci. Technol. **14**, L21 (1999).
[2] A. A. Darhuber, P. Schittenhelm, V. Holy, J. Stangl, G. Bauer, and G. Abstreiter, Phys. Rev. B **55**, 15 652 (1997).
[3] H. Sunamura, N. Usami, Y. Shiraki, and S. Fukatsu, Appl. Phys. Lett. **66**, 3024 (1995).
[4] O. G. Schmidt, C. Lange, and K. Eberl, Appl. Phys. Lett. **75**, 1905 (1999).
[5] See, e.g., O. G. Schmidt, U. Denker, K. Eberl, O. Kienzie, and F. Ernst, Appl. Phys. Lett. **77**, 2509 (2000).
[6] P. O. Nilsson, J. Kanski, J. V. Thordson, T. G. Andersson, J. Nordgren, J. Guo, and M. Magnusson, Phys. Rev. B **52**, R8643 (1995).
[7] S. Mankefors, P. O. Nilsson, J. Kanski, and K. Karlsson, Vacuum **49**, 181 (1998).
[8] S. Mankefors, P. O. Nilsson, J. Kanski, and K. Karlsson, Phys. Rev. B **58**, 10 551 (1998).
[9] P. O. Nilsson, S. Mankefors, and E. Lundgren, J. Alloys Compd. **286**, 31 (1999).
[10] S. Mankefors, P. O. Nilsson, J. Kanski, T. Andersson, K. Karlsson, A. Agui, C. Såthe, J. Guo, and J. Nordgren, Phys. Rev. B **61**, 5540 (2000).
[11] S. Mankefors, Appl. Surf. Sci. **166**, 313 (2000).
[12] A. Agui, C. Såthe, J.-H. Guo, J. Nordgren, S. Mankefors, P. O. Nilsson, J. Kanski, T. G. Andersson, and K. Karlsson, Appl. Surf. Sci. **166**, 309 (2000).
[13] W.-X. Ni and G. V. Hansson, Phys. Rev. B **42**, 3030 (1990).
[14] J. D. Denlinger, E. Rotenberg, T. Warwick, G. Visser, J. Nordgren, J.-H. Guo, P. Skytt, S. D. Kevan, K. S. McCutcheon, D. Shuh, J. Bucher, N. Edelstein, J. G. Tobin, and B. P. Tonner, Rev. Sci. Instrum. **66**, 1342 (1995).
[15] J. Nordgren, G. Bray, S. Cramm, R. Nyholm, J.-E. Rubensson, and N. Wassdahl, Rev. Sci. Instrum. **60**, 1690 (1989).
[16] W. Kohn and L. J. Sham, Phys. Rev. **140**, A1133 (1965).
[17] P. Hohenberg and W. Kohn, Phys. Rev. **136**, B864 (1964).
[18] D. M. Ceperley and B. J. Alder, Phys. Rev. Lett. **45**, 566 (1980).
[19] J. P. Perdew and A. Zunger, Phys. Rev. B **23**, 5048 (1981).
[20] B. Hamann, Phys. Rev. B **40**, 2980 (1989).
[21] X. Gonze, P. Käckell, and M. Scheffler, Phys. Rev. B **41**, 12 264 (1990).
[22] D. R. Hamann, M. Schlüter, and C. Chiang, Phys. Rev. Lett. **43**, 1494 (1979).
[23] G. B. Bachelet, D. R. Hamann, and M. Schlüter, Phys. Rev. B **26**, 4199 (1982).
[24] L. Kleinmann and D. M. Bylander, Phys. Rev. Lett. **48**, 1425 (1982).
[25] FHI94MD.CTH is based on FHI93CP, purchased from the Computational Physics Communications library in 1995. While the basic computational physics is the same, the changes of computational nature are extensive.
[26] R. Stumpf and M. Scheffler, Comput. Phys. Commun. **79**, 447 (1994).
[27] S. Mankefors, P. O. Nilsson, J. Kanski, and K. Karlsson, Phys. Rev. B **56**, 15 847 (1997).
[28] S. Mankefors, P. O. Nilsson, J. Kanski, and K. Karlsson, Vacuum **49**, 181 (1998).
[29] L. V. Azaroff, *X-Ray Spectroscopy* (McGraw-Hill, New York, 1974).